

Anonymous Referee #2

Summary

Cheung et al. conducted a set of ambient measurements from which they calculated size dependent volatility shrinkage factors (VSF) of aerosols in Guangzhou after heating to 300°C in a tandem differential mobility analyzer. Size-selected particles ranging from $D_m = 40$ to 300 nm were examined. Mass concentrations of OC and EC were also measured. Particles were classified as “completely volatile” (CV; $VSF \sim 0$), “high volatility” (HV; $VSF < 0.4$), “medium volatility” (MV; $0.4 < VSF < 0.9$) and “low volatility” (LV; $VSF > 0.9$). Three primary results are reported: (1) the number and volume fraction of CV particles decreases with increasing particle size, while the LV particle number and volume fractions increase with increasing diameter (2) size-resolved measurements combined with average diurnal patterns suggest that 40 nm CV and LV particles represent local, fresh emissions, whereas >80 nm HV and MV particles represent aged emissions. (3) A closure analysis of VHTDMA and OC/EC analyzer measurements suggests that organics comprise a significant fraction of the measured MV and LV. Overall, the results are interesting, but I suggest additional analysis of the data before I would support publication in ACP. In particular, I think it would be useful to present more of the OC/EC results to assist with, and expand on, the interpretation of the VHTDMA measurements.

Main Comments

1. In my opinion, the closure analysis -- which currently focuses on a comparison of $EC + OC_2 + OC_3 + OC_4$ versus $LV + MV$ -- is incomplete. The volatility resolved VHTDMA and OC/EC analyzer measurements should in principle allow for a more comprehensive closure/inter comparison study. Because the volatility fractions in both instruments are affected by the specific operation conditions, I think expanding on this subject in Section 3.3 would be interesting and possibly help with the interpretation of the VHTDMA measurements. I suggest that this subject be a major focus of a revised manuscript. For example:

- a) CV versus OC1*
- b) HV versus OC1 and/or OC2*
- c) MV and OC2 and/or OC3*

2. *I think the authors should plot and discuss campaign-average mass fractions of OC1, OC2, OC3, OC4 and EC to accompany the volume fractions of VM, CV, HV, MV and LV that are presented in Figure 6 and related discussion.*
3. *Similarly, the authors could plot time series and diurnal patterns of OC1, OC2, OC3, OC4 and EC mass fractions as is done in Figure 7 and related discussion of the volume fractions of VM, CV, HV, MV and LV.*

Response:

We thank the reviewer for the useful comments. Below please find our response to each of the points above. [Major changes to the manuscript are shown in blue.](#)

We have added the following new results in conjunction with the discussions of the VTDMA results:

- i) Time series and diurnal variations in OC and EC concentrations;
- ii) Meteorological conditions including wind speed, wind direction, temperature, and relative humidity;
- iii) Particle number size distribution from the SMPS; and
- iv) Back trajectory analysis

With the addition of the new materials, the subsections in the results and discussion section of the revised manuscript are re-organized:

- 3.1 Overview
- 3.2 Diurnal variations
- 3.3 Back trajectory analyses
- 3.4 New particle formation
- 3.5 Closure analysis for LV and MV residuals at 300 °C, OC and EC

The response below will focus on the new discussions related to the OC and EC data in addition to the main comments raised by the reviewer. Detailed discussions about the meteorological conditions can be found in item 1.2 of the major comments for Reviewer 1 or the revised manuscript.

1. For suggested closure b) and c), we would like to point out that LV, MV, and HV particles differ in the relative abundance of the volatile fraction over the non-volatile fraction at 300°C but not the volatility of the evaporated materials. On the other hand, OC₁, OC₂, OC₃ and OC₄ represent OC of different volatilities, as measured at different evaporation temperatures. Since the differentiation of LV, MV and HV relies on a different set of principles than the differentiation of OC₁, OC₂, OC₃ and OC₄, we do not think it useful to conduct any closure analysis related to b) and c).

We agree that it would be useful to carry out the suggested closure a) of CV versus OC₁ as proposed by the reviewer. However, a closure analysis between VM or CV and OC₁ was not conducted because there is a large uncertainty in the calculation of the vaporized mass (VM and CV). The estimation of the mass of vaporized materials (VM and CV) requires subtracting the volumes of LV and MV particles from the total particle volume, which was estimated by SMPS. However, unlike LV, MV, and HV particles, which had volume distributions peaking at diameters below 400 nm, the SMPS data suggest that the total volume almost always peaked at sizes above 400 nm. The calculation of VM and CV would involve large uncertainties due to the need to extrapolate the volume contributions of particles larger than 400 nm in size. Hence, we are not confident that one can draw meaningful conclusions from such analysis.

2. New materials added

2.1 Overview of OC/EC data

The time series of EC and OC concentrations and the OC/EC ratio during the campaign are shown in Fig. R1. OC concentrations ranged from 0.5 to 47.0 $\mu\text{g m}^{-3}$ with an average of $9.0 \pm 6.0 \mu\text{g m}^{-3}$, while EC concentrations ranged from 0.2 to 23.0 $\mu\text{g m}^{-3}$ with an average of $3.4 \pm 3.0 \mu\text{g m}^{-3}$. OC₁, the most volatile group among OC₁ to OC₄ in OC/EC analysis, accounted for one-third of the total carbon mass (Fig. R2). Similar to the number concentrations of MV particles (with an initial diameter of 80 nm and above) measured by the VTDMA at 300 °C, OC and EC mass correlated well with PM_{2.5}. The r^2 values of the correlations between OC and PM_{2.5} and between EC and PM_{2.5} are 0.8 and 0.7, respectively (Fig. R3).

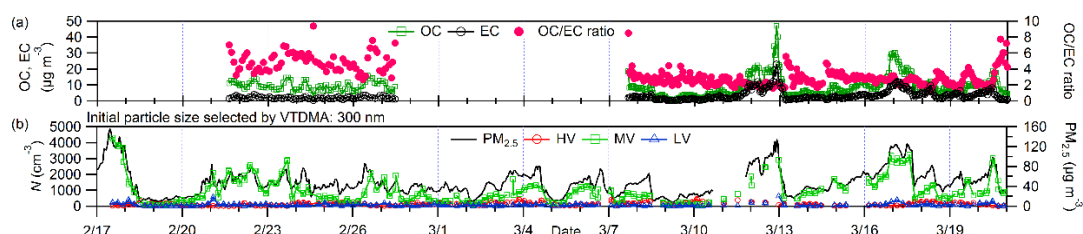


Fig. R1. Time series of (a) OC and EC concentrations and the OC/EC ratio, (b) number concentrations of HV, MV and LV particles having an initial diameter of 300 nm upon heating at 300 °C (left axis) and concentration of PM_{2.5} (right axis).

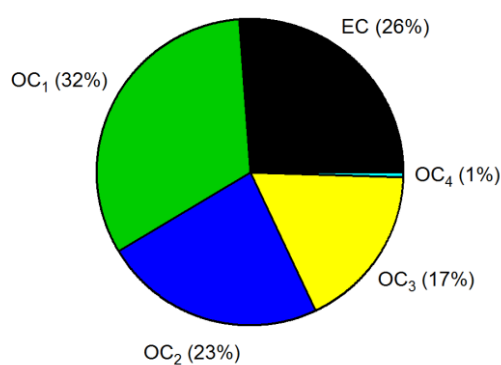


Fig. R2. Average mass fractions of EC, OC₁, OC₂, OC₃ and OC₄ in PM_{2.5}.

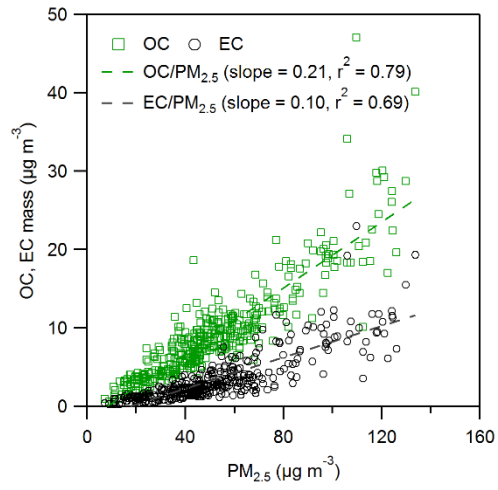


Fig. R3. Concentrations of OC and EC versus PM_{2.5}.

2.2 Comparison of the diurnal variations of OC/EC and VTDMA data

The diurnal variations in the mass fractions of OC and EC in PM_{2.5} are compared with the volume fractions of CV, HV residual, MV residual, LV residual and VM in particles of dry initial diameters of 40, 150 and 300 nm. The OC and EC data on Mar 12 and 17 were excluded since they were more than two standard deviations higher than those on other days. Subtle morning peaks between 06:00 and 10:00 were observed for the volume fraction of LV residuals (Fig. R4). A similar peak was observed for the mass fraction of EC in PM_{2.5} in the morning (Fig. R5). This suggests that LV particles may be related to the EC from vehicle emissions in the morning. This EC was relatively less aged and externally mixed with other volatile materials. In the late afternoon, LV residuals showed another peak between 17:00 and 19:00 whereas the mass fraction of EC in PM_{2.5} exhibited a minimum at 15:00, after which it increased continuously. The continuous increase in EC at night is likely related to the increase of heavy-duty diesel vehicles (Zhang et al., 2015), which was restricted during daytime (Bradsher, 2007).

Although OC₁ contributed to about half of the total OC mass, the diurnal variation in the mass fraction of OC in PM_{2.5} was driven by the total mass of OC₂, OC₃ and OC₄ (OC₂₋₄), which reached a minimum between 05:00 and 09:00 and increased until 19:00. OC can be attributed to both primary and secondary sources. The increased mass fraction of OC in PM_{2.5} and OC-to-EC ratio in the afternoon suggest that the sources of OC were less related to traffic but more to the aging and formation of secondary organic aerosols (Turpin et al., 1990; Chow et al., 1996). These OC₂, OC₃ and OC₄ may be highly oxygenated species or oligomers that are less volatile than primary or less oxygenated organics (Kalberber et al., 2004; Huffman et al., 2009).

It is interesting to note that the volume fraction of LV residuals and the *VFR* of MV particles at different sizes showed a dip in the afternoon (Fig. R4, third column from the left). The *VFR* of 40 nm MV particles showed a dip at 14:00 while those in 150 nm and 300 nm particles showed a dip at 15:00. The volume fraction of LV residuals in 150 nm and 300 nm particles reached a minimum at 13:00 and 15:00, respectively. Because EC decreased between 12:00 and 15:00, the increase in the volume fraction of LV residuals in 150 nm particles since 13:00 and the *VFR* of 40 nm MV particles

since 14:00 may be related to the increased presence of aged organics as well as the EC particles which aged via coagulation and condensation.

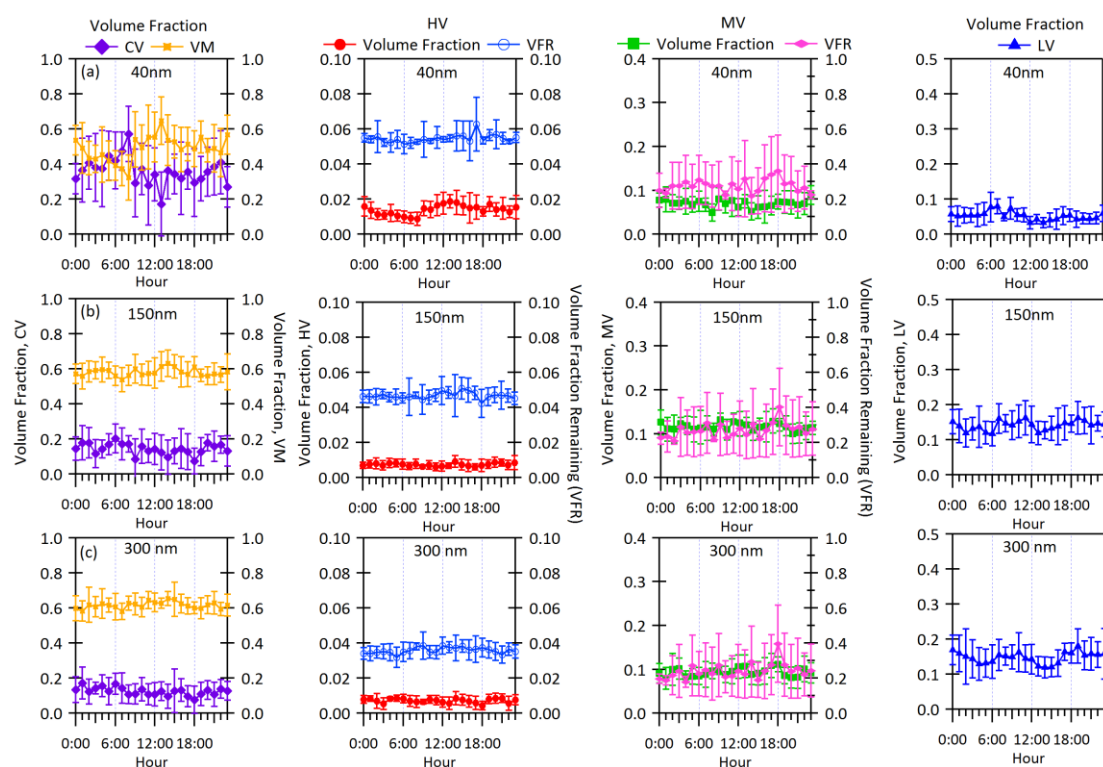


Fig. R4. Diurnal variations in volume fractions of (columns from left to right) CV, VM, HV residual, MV residual and LV residual in (a) 40 nm, (b) 150 nm and (c) 300 nm particles. Diurnal variations in the volume fraction remaining (*VFR*) of HV and MV particles are plotted on the right axis. Error bars represent one standard deviation.

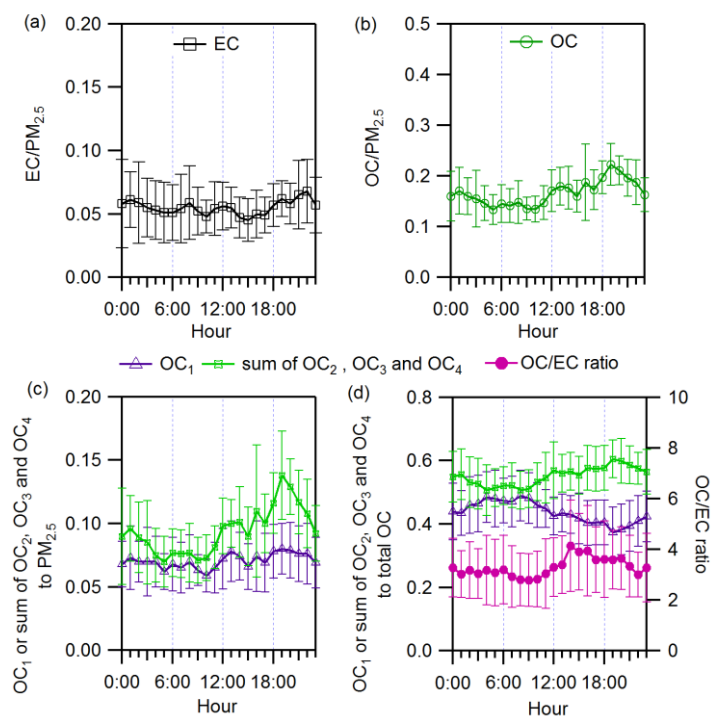


Fig. R5. Diurnal variations in the mass fractions of EC, OC, OC₁ and the sum of OC₂, OC₃ and OC₄ in PM_{2.5}, the ratio of OC to EC, mass fractions of OC₁ and the sum of OC₂, OC₃ and OC₄ to total OC in February and March. Error bars represent one standard deviation.

2.3 Back Trajectory Analysis

We calculated the 72 h back trajectories of the air masses arriving at the sampling site (23°00' N, 113°25' E) at 4 h intervals (at 00:00, 04:00, 08:00, 12:00, 16:00 and 20:00 local time, UTC +8) using the PC version of the HYSPLIT4 (Hybrid Single Particle Lagrangian Integrated Trajectory, version 4) model (Stein et al., 2015; Rolph, 2016). Archived meteorological data from the Global Data Assimilation System (GDAS) 1-deg was employed and the receptor height was set at 500 m above ground level (a.g.l.). The 191 back trajectories calculated were grouped into six clusters based on their spatial distribution (Fig. R6).

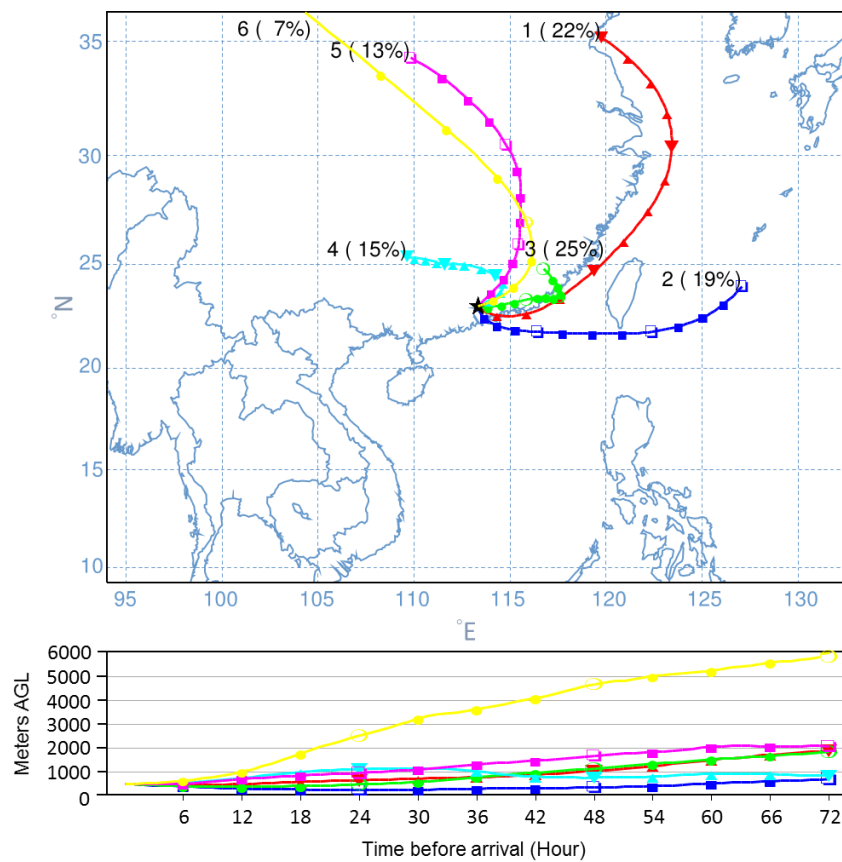


Fig. R6. Mean back trajectories of the six types of air masses arriving at the sampling site.

Overall, the sampling site was mostly affected by northwesterly and northeasterly air masses. Cluster 1 and 3 are coastal and continental air masses, respectively, although both originated from the northeast. Clusters 4, 5 and 6 represent continental air masses originating from the northwest. Cluster 2 is a group of maritime air masses originating from the East China Sea northeast or east of Guangzhou. While air masses in cluster 6 were transported at relatively high speeds and altitudes (over 3000 m a.g.l.), air masses in all the other clusters were transported at an altitude below 1500 m a.g.l. for over 40 h before arriving at the site. Nevertheless, air masses in cluster 6 only persisted for less than three days. Since the corresponding VTDMA and OC/EC data were sometimes unavailable, cluster 6 will be excluded from the following discussion.

The average PM_{2.5}, OC and EC concentrations associated with air masses from the northeast of Guangzhou (clusters 1, 2 and 3) were higher than those from the northwest (clusters 4 and 5, Table R1). Days associated with coastal and maritime air masses were more polluted than days associated with continental air masses for several reasons. First, south China as a region is often affected by the high pressure system moving eastward or southward from the continent out to sea in winter. When the maritime or coastal air streams entered from the southeast of the sampling site at Panyu, the atmosphere at the sampling site became more stable with low local wind speeds (e.g. the polluted days on Feb 17 and Mar 12, 16 and 17, Fig. R7 and R8). Local pollutants accumulated and the city was also affected by pollutants from the southeastern areas of the site (e.g. Shenzhen, Nansha and Dongguan). Second, land-sea breeze cycles were observed when the sampling site was under the influence of maritime air masses from Mar 18 to 20. During the day, southeasterly wind prevailed and the wind speed was higher. In the evening, the southeasterly wind was gradually replaced by a southwesterly or northwesterly wind and the wind speed decreased (Fig. R7). The cycle started again in the morning when the westerly wind was gradually replaced by southeasterly wind. Such land-sea breeze effects can result in an effective redistribution and accumulation of air pollutants within the PRD region (Lo et al., 2006).

Table R1. Summary of concentrations of PM_{2.5}, OC, EC and the ratio of OC to EC (OC/EC) in the five clusters.

	Cluster				
	Coastal	Maritime	Continental		
	1	2	3	4	5
Origin (to the site)	NE	NE/E	NE	NW	NW
PM _{2.5} (µg m ⁻³)	58.5 ± 24.4	58.9 ± 30.9	47.5 ± 28.4	33.9 ± 15.9	33.8 ± 19.3
OC (µg m ⁻³)	10.8 ± 6.01	10.84 ± 7.22	10.13 ± 6.89	5.51 ± 3.3	7.32 ± 2.75
EC (µg m ⁻³)	4.38 ± 2.97	4.98 ± 4.21	3.43 ± 3.12	1.8 ± 0.98	2.46 ± 0.59
OC/EC	2.83 ± 1.05	2.62 ± 1.03	3.65 ± 1.6	3.18 ± 1.26	2.94 ± 0.73

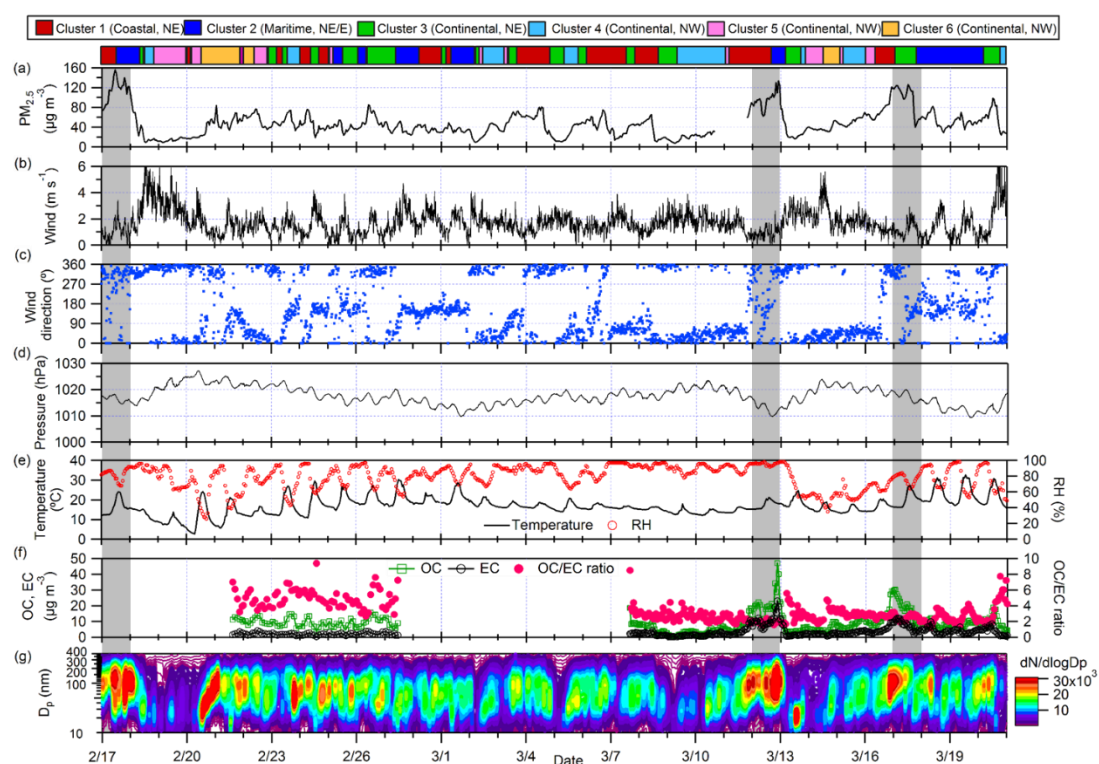


Fig. R7. Overview of major meteorological parameters, PM_{2.5}, OC and EC concentrations, OC/EC ratio and particle number size distributions in the campaign. Air mass clusters are depicted at the top and the shaded areas indicate days with daily-averaged PM_{2.5} concentrations exceeding 95 µg m⁻³.

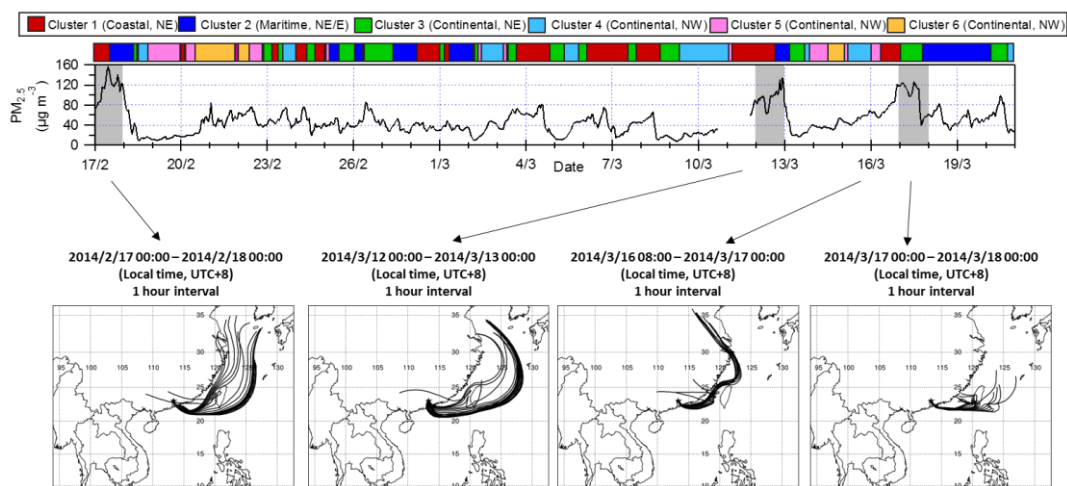


Fig. R8. Time series of $PM_{2.5}$ concentrations and 72 h back trajectories at hourly intervals on Feb 17, and Mar 12, 16 and 17.

Furthermore, $PM_{2.5}$ in the northeastern parts of China can exceed $200 \mu\text{g m}^{-3}$ due to both enhanced emissions from coal combustion for heating and poor dispersion during wintertime (Gu et al., 2014). Under the influence of the prevailing northerly or northeasterly wind in China, these pollutants were often transported to southern China and the East China Sea (Chen et al., 2012). Pollutants might also have accumulated when the maritime air masses spent about two days across Taiwan and the coast of south China. In contrast, continental air masses in cluster 5 moved slightly faster, and were often associated with the cold front period during which the local wind speed and pressure increased but the temperature decreased (Fig. R7). As the cold air masses passed through the city, dispersion and clearance of pollutants were promoted, resulting in lower $PM_{2.5}$ concentrations (Tan et al., 2013). Therefore, unlike in other coastal cities like Hong Kong (Lee et al., 2013), in Panyu maritime air masses could lead to more severe pollution than the continental ones in winter.

The five clusters were further analyzed to study the influence of air mass history on aerosol volatility. The number fractions of CV, HV, MV and LV of the six selected diameters in VTDMA measurements are regrouped based on the clusters as shown in Fig. R9. The total number fractions of the non-volatile residuals (sum of HV, MV and LV) were similar in all clusters. Maritime air masses (cluster 2) had a slightly higher fraction of LV particles while continental air masses originating from the northwest of the site (clusters 4 and 5) had a higher fraction of HV particles. Although the air masses

in clusters 1 and 5 originated from farther away and traveled at relatively higher speeds than those in clusters 2, 3 and 4, all clusters involved transport at low altitudes (below 1500 m) for over 40 h, likely due to the generally lower mixing heights in winter. Therefore, aerosols in these air masses were all well-aged upon arrival (Wehner et al., 2009). This could be another reason for the lack of size dependence of the number, volume fractions and diurnal variation for particles larger than 80 nm. When the transported air masses mixed with local pollutants, the size dependence of the number fractions of different volatility groups as well as the aging of local emissions was further reduced.

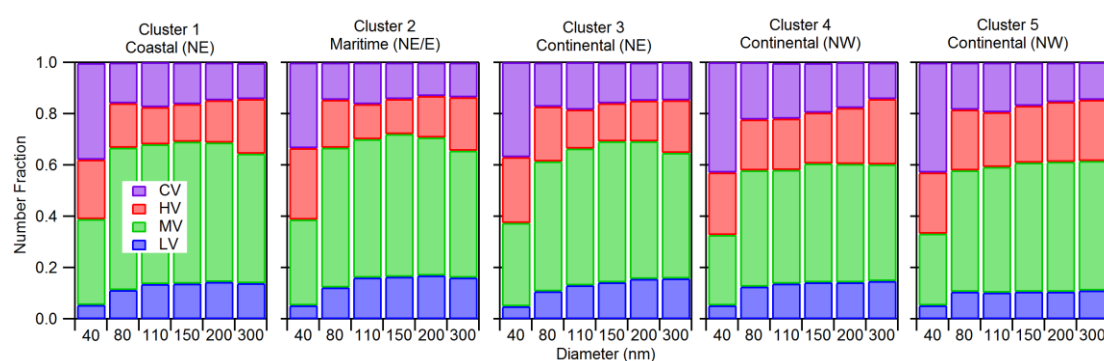


Fig. R9. Average number fractions of CV, HV, MV and LV particles in clusters 1 to 5 at different selected diameters.

We also examine at the volatility shrinkage factor (*VSF*) distributions of 40 nm, 110 nm and 300 nm particles upon heating at 300 °C (Fig. R10). Log-normal fittings with a three-peak solution were applied to the distributions. The average *VSF* modes of the peaks were located at 0.38 ± 0.021 (peak 1), 0.60 ± 0.066 (peak 2) and 0.95 ± 0.007 (peak 3), respectively. The standard deviation of the corresponding normal distribution (σ) of peak 3 was the smallest among the three peaks ($\sigma < 0.1$). For the same particle size, the *VSF* distributions in the *VSF* range between 0.3 and 0.8 in cluster 5 was relatively more uni-modal than those of other clusters (Fig. R10b and R10c). This suggests that the composition in cluster 5 was more homogeneous. Cluster 1 also consisted of long-range transported air masses but they likely passed through areas that are more polluted and mixed with different types of pollutants. Note that the fractions of HV, MV and LV have been traditionally defined based on the values of *VSF*, i.e. $HV < 0.4$; $0.4 < MV < 0.9$; $LV > 0.9$ (Wehner et al., 2009). The *VSF* distributions above suggest that these definitions using $VSF = 0.4$ and 0.9 may need to be re-visited in the future.

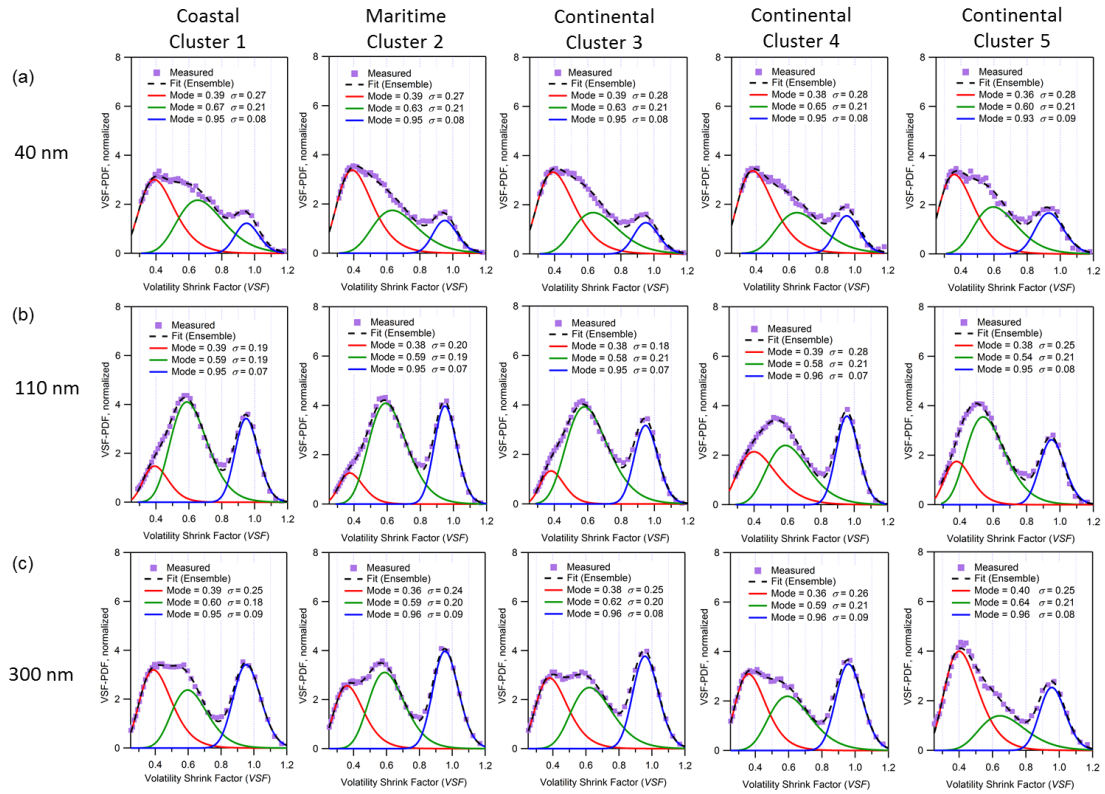


Fig. R10. Normalized probability distribution function of the volatility shrink factor (VFSF) in different clusters. Solid and dotted lines are the peaks fitted with log-normal function and the ensemble distributions, respectively.

3. Please refer to item 2.

Minor/Technical Comments

4. *It is not clear to me how understand the difference between “Volatile Materials” (VM) are defined. I assumed that “VM” becomes “CV” after heating to 300°C, but this does not seem to be the case because separate volume fractions of “VM” and “CV” are presented in Figures 6 and 7. Please clarify the definition of VM.*

Response:

VM and CV differ by how the evaporated materials mix with the non-volatile materials. VM refers to the volatile materials that are internally mixed with (or coated on) the non-volatile materials while CV refers to the volatile materials that are externally mixed with particles containing the non-volatile materials. Upon heating, VM evaporated, leaving behind HV, MV, or LV residuals. Evaporation of VM alone does not change the total number concentrations of particles. In contrast, CV particles evaporated completely without leaving any residuals behind. It reduced the total particle number concentrations.

On page 25275 of the original manuscript, Section 2.1.2, line 19 onwards, we mentioned:

Figure 2 illustrates how thermal treatment in the VTDMA affects the size distributions of the ambient aerosols. At each selected diameter D_0 (and at each temperature) in DMA₁ in the VTDMA, the particles include CV particles (purple) and **LV, MV and HV particles that have VM (orange) internally mixed with the LV (blue), MV (green) and HV (red) residuals**. After heating, the remaining particles would form LV, MV and HV residuals without any CV or VM.

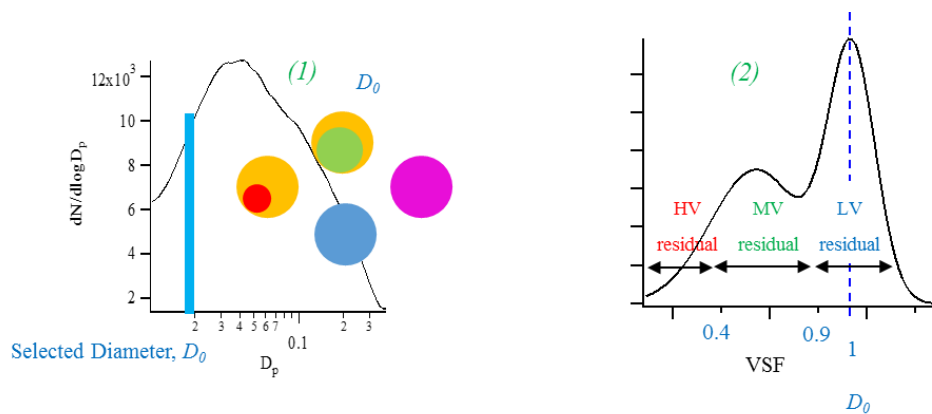


Fig. 2. Examples of particle size distributions of (a) ambient aerosols before entering DMA₁ and (b) residuals of the size-selected particles (D_0) after heating. The left and right distributions correspond to (1) and (2) in Fig. 1 respectively. Residuals are divided into three groups—LV (blue), MV (green) and HV (red)—based on their *VSF*. CV (purple) and VM (orange) are completely vaporized and hence not measured as residuals. VM appears as coating for illustration purposes only. It does not necessarily reflect the morphology of the particles.

In the revised manuscript, CV and VM are clearly defined in the methodology section instead of the introduction section. VM refers to volatile materials internally mixed with non-volatile ones while CV refers to volatile materials externally mixed with non-volatile materials.

Revised Methodology (Section 2.1.2):

...The *VSF* is also used to divide the particles into three groups, namely the low volatility (LV), medium volatility (MV) and high volatility (HV) particles. In this study, we focus on the measurements made at 300 °C. The *VSF* ranges for LV, MV and HV particles upon heating at 300 °C are above 0.9, between 0.4 and 0.9 and below 0.4, respectively (Fig. 2) (Wehner et al., 2004; Wehner et al., 2009). The LV particles are assumed to represent EC particles externally mixed with the volatile materials, while the MV and HV particles are assumed to represent EC particles internally mixed with volatile materials. While the volatile materials in the MV and HV particles are referred to as VM, those exist as external mixtures with the LV, MV and HV particles are referred to as completely vaporized (CV) particles. The CV particles evaporate completely without leaving behind any residuals at 300 °C.

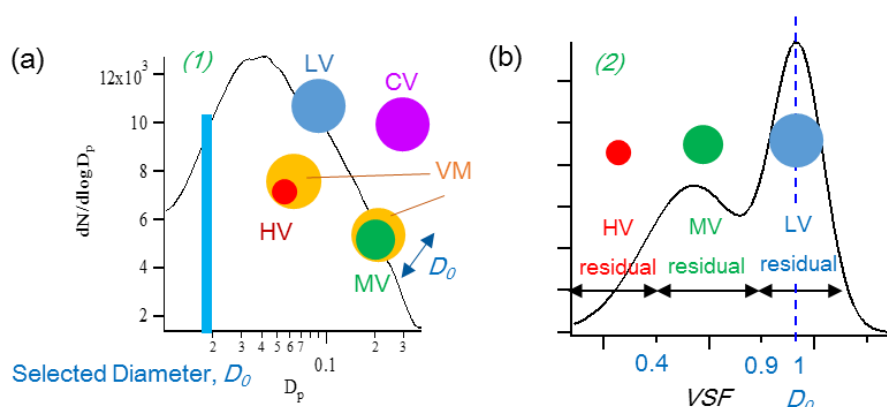


Fig. 2. Examples of particle size distributions of (a) ambient aerosols before entering DMA_1 and (b) residuals of the size-selected particles (D_0) after heating. The left and right distributions correspond to (1) and (2) in Fig. 1 respectively. Residuals are divided into three groups—LV (blue), MV (green) and HV (red)—based on their *VSF*. CV (purple) and VM (orange) are vaporized and hence not measured as residuals. VM appears as coating for illustration purposes only. It does not necessarily reflect the morphology of the particles.

5. *OC₂, OC₃ and OC₄ are never defined in the manuscript.*

Response:

On page 25276 of the original manuscript, line 19 – 22, we mentioned:

“The OC/EC Analyzer adopts the ACE-Asia protocol (a NIOSH-derived protocol), where OC evaporates at four set temperatures of 310, 475, 615 and 870 °C, and EC is combusted at temperature above 550 °C (Schauer et al., 2003). Based on volatility and refractoriness, the OC contents are named OC₁ to OC₄ with OC₁ being most volatile”

We agree that the definitions did not explicitly link the terms and the heating temperatures. The revised description is shown below.

Revised:

The OC/EC analyzer adopts the ACE-Asia protocol (a NIOSH-derived protocol), where OC evaporates at four set temperatures of 310 °C, 475 °C, 615 °C and 870 °C **with pure helium (He) as the carrier gas**, and EC is combusted at temperatures **between 550 °C and 870 °C under He and 2% oxygen** (O₂, Schauer et al., 2003; Wu et al., 2012). The OC contents are named OC₁ to OC₄ **based on the temperature protocol of the OC/EC analyzer (Table R2). The mass of EC determined at different temperatures will be grouped together for discussions.**

Table R2. Temperature (T) and residence time (RT) protocol of the semi-continuous Sunset OC/EC analyzer (Wu et al., 2012)

Carbon Fraction	Carrier Gas	T (°C)	RT (s)
OC ₁	He	310	80
OC ₂		475	60
OC ₃		615	60
OC ₄		870	90
EC ₁	He + 2% O ₂	550	45
EC ₂		625	45
EC ₃		700	45
EC ₄		775	45
EC ₅		850	45
EC ₆		870	45

6. *What is the residence time in the heated section of the VTMDA, and how sensitive are the HV/MV/LV classifications to the residence time?*

Response:

The heating tube was a 1/2", 80 cm long stainless steel tube with an inner diameter of 8 mm. With a sample flow rate of 1 L min⁻¹, the resulting residence time in the heated section of the VTMDA was 2.4 s. The estimated aerosol velocity on the center line was 0.33 m s⁻¹. Compared to the residence time of 0.3 s to 1 s in other VTMDA systems (e.g. Brooks et al., 2002; Philippin et al., 2004; Villani et al., 2007), the residence time in our VTMDA is assumed to be long enough for the volatile materials to be effectively vaporized. After leaving the heating tube, the flow entered a heat exchanger measuring 30 cm in length to ensure sufficient cooling before entering DMA₂. The relevant information is added to the methodology section.

Revised, Page 25275 of the original manuscript, line 5 onwards:

Afterwards, the monodisperse aerosols were directed via path (b) to a heated tube for volatility measurement (V-Mode) sequentially at 25, 100 and 300 °C. The heating tube was a 1/2", 80 cm long stainless steel tube with an inner diameter of 8 mm. With a sample flow rate of 1 L min⁻¹, the resulting residence time in the heated section of the VTMDA was 2.4 s. The estimated aerosol velocity on the center line was 0.33 m s⁻¹. Compared to the residence time of 0.3 s to 1 s in other VTMDA systems (e.g. Brooks et al., 2002; Philippin et al., 2004; Villani et al., 2007), the residence time in our VTMDA is assumed to be long enough for the volatile materials to be effectively vaporized. After leaving the heating tube, the flow entered a heat exchanger measuring 30 cm in length to ensure sufficient cooling before entering DMA₂.

7. **P25275, L8-10:** *The authors state: “Upon heating at 100 °C and beyond, volatile components of the particle such as sulfate, nitrate and volatile organics vaporize”. Please plot VSF (at 300°C) of ammonium sulfate, perhaps as a supplemental figure, over a few sizes ranging from 40 nm to 300 nm. I would not have thought that ammonium sulfate completely vaporizes at only 300°C.*

Response:

In a number of earlier studies, ammonium sulfate test aerosols were found to volatilize at temperatures between 160 °C and 280 °C (Table R3). The volatilization temperature of the tested aerosols varies with the initial diameter of the aerosols and their residence time in the heated section. In this work, the residence time in the heated section was 2.4 s, hence we believe that ammonium sulfate would be completely vaporized upon heating at 300 °C in the VTDMA. We did not mean to claim that ammonium sulfate would be completely vaporized at 100 °C in the original sentence (“Upon heating at 100 °C and beyond...”). The sentence is revised to avoid confusion.

Table R3. Volatilization temperature of ammonium sulfate test aerosols in the VTDMA (Villani et al., 2007)

	O'Dowd et al. (1992)	Philippin et al. (2004)	Burtscher et al. (2001)	Brooks et al. (2002)	Villani et al. (2007)
Volatilization temperature	280 °C	180 °C	180 °C	235 °C	160 to 180 °C

Revised, Page 25275 of the original manuscript, line 8 – 10:

Upon heating at 100 °C and **above**, volatile components of the particle such as sulfate, nitrate and volatile organics would vaporize **at different temperatures depending on their volatilities**.

References

- Bradsher, K.: <http://www.nytimes.com/2007/12/08/world/asia/08trucks.html>, 2007.
- Brooks, B. J., Smith, M. H., Hill, M. K., and O'Dowd, C. D.: Size-differentiated volatility analysis of internally mixed laboratory-generated aerosol, *Journal of Aerosol Science*, 33, 555-579, 2002.
- Burtscher, H., Baltensperger, U., Bukowiecki, N., Cohn, P., Hüglin, C., Mohr, M., Matter, U., Nyeki, S., Schmatloch, V., Streit, N., and Weingartner, E.: Separation of volatile and non-volatile aerosol fractions by thermodesorption: instrumental development and applications, *Journal of Aerosol Science*, 32, 427-442, 2001.
- Chen, B., Du, K., Wang, Y., Chen, J., Zhao, J., Wang, K., Zhang, F., and Xu, L.: Emission and transport of carbonaceous aerosols in urbanized coastal areas in China, 2012. 2012.
- Chow, J. C., Watson, J. G., Lu, Z., Lowenthal, D. H., Frazier, C. A., Solomon, P. A., Thuillier, R. H., and Magliano, K.: Descriptive analysis of PM_{2.5} and PM₁₀ at regionally representative locations during SJVAQS/AUSPEX, *Atmos. Environ.*, 30, 2079-2112, 1996.
- Gu, J., Du, S., Han, D., Hou, L., Yi, J., Xu, J., Liu, G., Han, B., Yang, G., and Bai, Z.-P.: Major chemical compositions, possible sources, and mass closure analysis of PM_{2.5} in Jinan, China, *Air Quality, Atmosphere & Health*, 7, 251-262, 2014.
- Lee, B. P., Li, Y. J., Yu, J. Z., Louie, P. K. K., and Chan, C. K.: Physical and chemical characterization of ambient aerosol by HR-ToF-AMS at a suburban site in Hong Kong during springtime 2011, *Journal of Geophysical Research: Atmospheres*, 118, 8625-8639, 2013.
- Lo, J. C. F., Lau, A. K. H., Fung, J. C. H., and Chen, F.: Investigation of enhanced cross-city transport and trapping of air pollutants by coastal and urban land-sea breeze circulations, *Journal of Geophysical Research: Atmospheres*, 111, n/a-n/a, 2006.
- O'Dowd, C. D., Jennings, S. G., Smith, M. H., and Cooke, W.: A high temperature volatility technique for determination of atmospheric aerosol composition, *Journal of Aerosol Science*, 23, Supplement 1, 905-908, 1992.
- Philippin, S., Wiedensohler, A., and Stratmann, F.: Measurements of non-volatile fractions of pollution aerosols with an eight-tube volatility tandem differential mobility analyzer (VTDMA-8), *Journal of Aerosol Science*, 35, 185-203, 2004.
- Rolph, G. D.: Real-time Environmental Applications and Display sYstem (READY) Website (<http://www.ready.noaa.gov>). NOAA Air Resources Laboratory, College Park, MD., 2016.
- Schauer, J. J., Mader, B. T., Deminter, J. T., Heidemann, G., Bae, M. S., Seinfeld, J. H., Flagan, R. C., Cary, R. A., Smith, D., Huebert, B. J., Bertram, T., Howell, S.,

- Kline, J. T., Quinn, P., Bates, T., Turpin, B., Lim, H. J., Yu, J. Z., Yang, H., and Keywood, M. D.: ACE-Asia intercomparison of a thermal-optical method for the determination of particle-phase organic and elemental carbon, *Environmental Science & Technology*, 37, 993-1001, 2003.
- Stein, A. F., Draxler, R. R., Rolph, G. D., Stunder, B. J. B., Cohen, M. D., and Ngan, F.: NOAA's HYSPLIT Atmospheric Transport and Dispersion Modeling System, *Bulletin of the American Meteorological Society*, 96, 2059-2077, 2015.
- Tan, H. B., Yin, Y., Gu, X. S., Li, F., Chan, P. W., Xu, H. B., Deng, X. J., and Wan, Q. L.: An observational study of the hygroscopic properties of aerosols over the Pearl River Delta region, *Atmos. Environ.*, 77, 817-826, 2013.
- Turpin, B. J., Cary, R. A., and Huntzicker, J. J.: An In Situ, Time-Resolved Analyzer for Aerosol Organic and Elemental Carbon, *Aerosol Science and Technology*, 12, 161-171, 1990.
- Villani, P., Picard, D., Marchand*, N., and Laj, P.: Design and Validation of a 6-Volatility Tandem Differential Mobility Analyzer (VTDMA), *Aerosol Science and Technology*, 41, 898-906, 2007.
- Wehner, B., Philippin, S., Wiedensohler, A., Scheer, V., and Vogt, R.: Variability of non-volatile fractions of atmospheric aerosol particles with traffic influence, *Atmos. Environ.*, 38, 6081-6090, 2004.
- Wehner, B., Berghof, M., Cheng, Y. F., Achtert, P., Birmili, W., Nowak, A., Wiedensohler, A., Garland, R. M., Pöschl, U., Hu, M., and Zhu, T.: Mixing state of nonvolatile aerosol particle fractions and comparison with light absorption in the polluted Beijing region, *Journal of Geophysical Research: Atmospheres*, 114, D00G17, 2009.
- Wu, C., Ng, W. M., Huang, J. X., Wu, D., and Yu, J. Z.: Determination of Elemental and Organic Carbon in PM_{2.5} in the Pearl River Delta Region: Inter-Instrument (Sunset vs. DRI Model 2001 Thermal/Optical Carbon Analyzer) and Inter-Protocol Comparisons (IMPROVE vs. ACE-Asia Protocol), *Aerosol Science and Technology*, 46, 610-621, 2012.